Nano-light-emitting-diodes based on InGaN mesoscopic structures for energy saving optoelectronics

M. Mikulics, A. Winden, M. Marso, A. Moonshiram, H. Lüth, D. Grützmacher, and H. Hardtdegen

Citation: Applied Physics Letters **109**, 041103 (2016); doi: 10.1063/1.4960007
View online: http://dx.doi.org/10.1063/1.4960007
View Table of Contents: http://scitation.aip.org/content/aip/journal/apl/109/4?ver=pdfcov
Published by the AIP Publishing

Nano-light-emitting-diodes based on InGaN mesoscopic structures for energy saving optoelectronics

M. Mikulics,[1,2] A. Winden,[3] M. Marso,[4] A. Moonshiram,[4] H. Lüth,[1,2] D. Grützmacher,[1,2] and H. Hardtdegen[1,2]
[1]*Peter Grünberg Institute (PGI-9) Forschungszentrum Jülich GmbH, D-52425 Jülich, Germany*
[2]*Jülich Aachen Research Alliance, JARA, Fundamentals of Future Information Technology, D-52425 Jülich, Germany*
[3]*Robert Bosch GmbH, D-72760 Reutlingen, Germany*
[4]*Faculté des Sciences, de la Technologie et de la Communication, Université du Luxembourg, L-1359 Luxembourg, Luxembourg*

(Received 19 May 2016; accepted 17 July 2016; published online 26 July 2016)

Vertically integrated III-nitride based nano-LEDs (light emitting diodes) were designed and fabricated for operation in the telecommunication wavelength range in the (p-GaN/InGaN/n-GaN/sapphire) material system. The band edge luminescence energy of the nano-LEDs could be engineered by tuning the composition and size of the InGaN mesoscopic structures. Narrow band edge photoluminescence and electroluminescence were observed. Our mesoscopic InGaN structures (depending on diameter) feature a very low power consumption in the range between 2 nW and 30 nW. The suitability of the technological process for the long-term operation of LEDs is demonstrated by reliability measurements. The optical and electrical characterization presented show strong potential for future low energy consumption optoelectronics. *Published by AIP Publishing*. [http://dx.doi.org/10.1063/1.4960007]

Future energy saving optoelectronics including nano-LEDs (light emitting diodes) will be based on nanowires and mesoscopic structures.[1–3] Such structures are the key also for highly secure and ultrafast optoelectronics[4,5] as well as quantum dot based nano-photonics.[6,7] There is an especially strong need to develop such emitting sources for room temperature operation and at the wavelengths used for telecommunication. To this end, they must be fully compatible with established communication systems.[8] The InGaN alloy is especially suitable since it can be tailored to emit in the energy range between ~0.7 eV and ~3.4 eV solely by tuning the composition and benefits from the exceptional robustness[9] of GaN-based systems against mechanical, thermal, and radiative stress. The energy spectrum includes the important telecom windows used for long-range telecommunication (wavelengths around 1300 nm and around 1550 nm). Additionally, III-nitride semiconductors are well suitable for ultrafast optoelectronics. This has been confirmed by the fabrication of picosecond and sub-picosecond operated metal–semiconductor–metal photodetectors (MSM PDs) on low-temperature-grown GaN[10] as well as with their implementation into a monolithically integrated optoelectronic circuit.[11] Beside the suitable choice for the semiconductor emitter, major challenges are the whole nano-LED integration technology and especially the contacts for reliable long term operation. The top contact (including the highly p-doped GaN contact layer[12]) should be highly electrically conductive, optically transparent, thermally and mechanically stable, and simple to fabricate. The nano-LEDs should be well-positioned and should exhibit the least possible structural defects at which non-radiative recombination processes often occur. Such processes lead to a heating of the structures and to degradation, which impedes long-term stability. We chose the same bottom-up procedure[13] to define the emitting nanostructure's position by selective area growth[14] as reported for InN nanostructures. In contrast, here, we center on InGaN nano- and mesostructured arrays. They are obtained without any etching-related damage and are, in addition, of high crystalline perfection because the strain present between GaN and InGaN can be more easily relaxed directly during the growth of the nano- or mesostructures. The nano-LEDs were integrated into a vertical device layout suitable for DC testing and future high-frequency operation. Transparent Ni/Au contacts were employed, the annealing procedure of which was carefully optimized for long-term operation.

Figure 1 presents a principal schematic of the integration technology of a single p-GaN/InGaN/n-GaN nanopyramid. An n-doped GaN on sapphire template is covered with a SiO_2 layer in which holes are prepared by e-beam lithography and successive reactive ion etching (RIE) for selective area growth (Figure 1(a)). InGaN nanopyramids are deposited selectively in the apertures of the mask. As sketched in Figure 1(b), the nanostructures are contained within the mask at first during growth and then eventually exceed it forming the nanopyramids observed. They are subsequently capped with p-GaN as demonstrated in Figure 1(c). Figure 1(d) depicts the recessed Ohmic bottom contacts after various lithography, dry etching, and annealing steps as well as the thin semi-transparent metallic Ni/Au top contact. In order to realize the mesoscopic sized nano-LEDs emitting within the telecom band, we started with the site-controlled growth of InGaN nanostructures via catalyst-free selective-area MOVPE.[13,14] The initial point for selective area growth were uniform and smooth n-doped GaN layers of at least 1.3 μm thickness on sapphire (c-plane) masked with a 50 nm thick SiO_2 layer. The manufacturing process was optimized with respect to the mask pattern in order to be able to fabricate individually addressable InGaN nanopyramid based nano-LEDs. To this end, a hexagonally arranged array of openings was defined by electron beam lithography followed by reactive ion etching (RIE) with trifluoromethane (CHF_3) gas with a separation

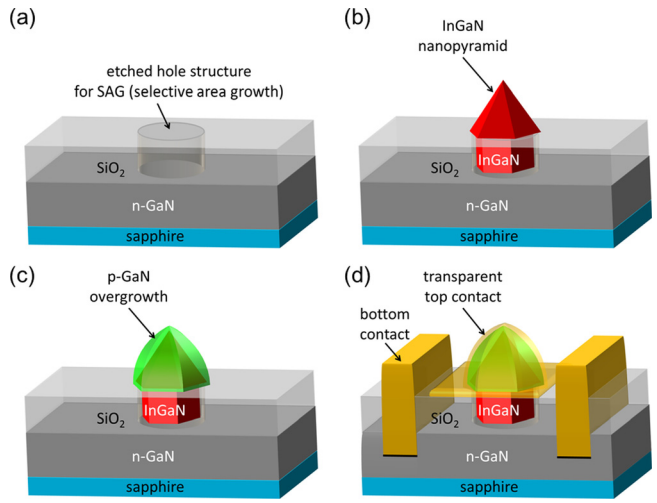

FIG. 1. Principal schematics of the integration technology of a single p-GaN/In GaN/n-GaN nanopyramid. (a) After E-beam lithography and RIE-hole pattern transfer in SiO_2 layer/mask, (b) after selective area growth/MOVPE of InGaN nanopyramids, (c) after selective p-GaN overgrowth by MOVPE, (d) recessed Ohmic bottom contacts were processed by various lithography, dry etching, and annealing steps. A thin semi-transparent metallic film of Ni/Au was used for the top contact.

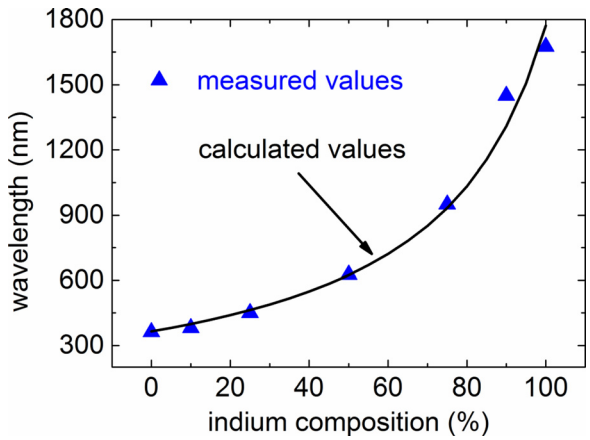

FIG. 2. Dependence of the PL emission wavelength for InGaN nanopyramids (diameter: 100 nm) on the In composition. The line presents calculated values using Equation (1),[19] 0.25 as the parameter b and converting energy into wavelength. The emission wavelength can be tuned from the UV range (GaN–365 nm) through the visible up to the near infrared range by controlling the TMIn to total group III molar flow ratio. When using an In composition of close to 90%, emission is achieved in the technologically important telecommunication wavelength range.

distance fixed to 3 μm. The bottom hole diameter was varied from 20 nm to 100 nm. All samples were grown by MOVPE in an AIX 200/4 RF-S horizontal flow reactor (AIXTRON) using N_2 as the carrier gas to transport the precursors triethyl gallium (TEGa) and trimethyl indium (TMIn) for the In containing alloy.[15–18] Growth parameters were employed which were tuned with respect to the highest possible selectivity resulting in a reactor pressure of 400 mbar, a growth temperature of 650 °C, and an NH_3 to group III precursor molar flow ratio of 22 000. The composition of the InGaN nanostructures was varied by changing the TMIn molar flow from 0.712 μmol/min to 6.4 μmol/min at a constant total group III precursor molar flow of 7.12 μmol/min. P-doped GaN capped the nanostructures. After this optimization, the growth time was varied in order to study the evolution of nanostructures with respect to their morphology and their optical properties.[8] Details on the growth experiments will be reported separately. A series of samples with varying InGaN composition and with a constant hole diameter of 100 nm were investigated by micro-photoluminescence (PL) first. The recorded emission wavelength for this series is presented in Figure 2. A similar experimental observation was reported for InGaN *layers* for example, by Vurgaftman *et al.*[19] There the emission wavelength at room temperature correlates with the band gaps of the alloys. It obeys the following equation for the whole alloy composition range:

$$E(\mathrm{In}_x\mathrm{Ga}_{1-x}\mathrm{N}) = xE(\mathrm{InN}) + (1-x)E(\mathrm{GaN}) - bx(1-x), \quad (1)$$

where E(X) denotes the energy gap of the compound X, x the In content in the ternary alloy, and b renders the deviation from a linear interpolation (virtual-crystal approximation). "b" is also called the bowing parameter. Its physical origin can be traced to dis-order effects created by the presence of cations of a different size.[19] The experimental data reported are based on monocrystalline layers. These experimental results correlate well with theoretical values based on work by Pelá *et al.*[20] using the LDA-1/2 method (local density approximation) and which constitutes a better fit to experimental data than that published earlier by Ferreira *et al.*[21] Pelá combined first-principles calculations within the LDA-1/2 approach with the generalized quasi-chemical approach (GQCA) including dis-order and compositional effects. Their work also includes the approximation of the self-energy of excitations in semiconductors. It provides effective masses as well as energy band structures and band gap parameters in nearly ideal agreement with experimental results reported previously. Our nanostructures also exhibit a similar dependence of emission wavelength on the In composition. The room temperature emission energy may not be identical to the band gap of the nanostructures themselves but is most certainly near band edge luminescence and could additionally be influenced by deep level donor centers. Even though we cannot attribute the room temperature photoluminescence wavelength to the band gap energy with certainty, its control by changing the indium composition is important for applications independent of its origin and can also be described by Equation (1). The experimental data for our nanostructures with a diameter of 100 nm fit quite well to those calculated by the above equation if 0.25 is employed as the factor b relating to a deviation from a linear interpolation between the respective band gaps of the binary compounds InN and GaN for the alloy. This small bowing parameter could be attributed to the difference in strain/dis-order in our nanostructures in comparison to more disturbed layers (i.e., bulk materials). The experimental data presented here demonstrate that the wavelength was tunable from the UV range (GaN–365 nm) through the visible up to the near infrared range by controlling the TMIn to total group III molar flow ratio. When using an In composition of close to 90%, emission is achieved in the technologically important telecommunication wavelength range. This ratio/composition is employed for the subsequent experiments.

Next, the hexagonally arranged p-GaN/$In_{0.9}Ga_{0.1}N$ nanopyramid quantum dots were integrated into a device layout for DC testing and future high-frequency operation. The fabrication process was already described earlier.[8] After mesa isolation, bottom contacts were defined by optical lithography and, subsequently, Ar-ion beam etching (IBE) was used to remove the SiO_2 mask layer. This technology is sensitive to etching parameters and must be carefully optimized to minimize surface roughening/damage and to reduce detrimental in-depth defects due to channeling. Subsequently—after metallization with Ti/Al/Ni/Au—bottom contacts were annealed in nitrogen ambient under optimized temperature to prevent InGaN nanostructure degradation. Transparent top contacts Ni/Au[22] were deposited on top of the p-GaN/$In_{0.9}Ga_{0.1}N$ nanopyramids and subsequently treated with an optimized thermal annealing process. Additionally, the entire surrounding surface area (except for the mesa with bottom and top contacts) was coated with a 200 nm SiO_2 layer to prevent leakage currents. In the last step, the nano-LED device based on InGaN nanostructures was connected to contact pads (Ti/Au) for DC testing and future RF operation by employing optical lithography and a lift-off process. An SEM micrograph of the fully integrated nano-LED structure is presented in Figure 3.

Arrays of hexagonally arranged nano-LEDs with a hole diameter of 20 nm were characterized by micro electroluminescence (EL). A mapping (Figure 4) was carried out for the sake of statistics on the one hand for the evaluation of the effectiveness as well as the reproducibility of the optimized integration process on the other hand. The micro EL mapping intensity was recorded by an InGaAs detector and spectrally analyzed with the help of a RENISHAW spectrometer. All nano-LEDs exhibit EL in the same intensity range. Typical/representative full EL spectra are presented in Figure 5.

A systematic red shift of emission wavelength with decreasing structure size is observed (Figure 5). This observation is—at a first glance—rather counterintuitive. However, as long as the structure size does not approach the dimensions at which quantum confinement effects are to be expected, the dimension of the mesostructures should not affect the emission wavelength. However, it has been observed for

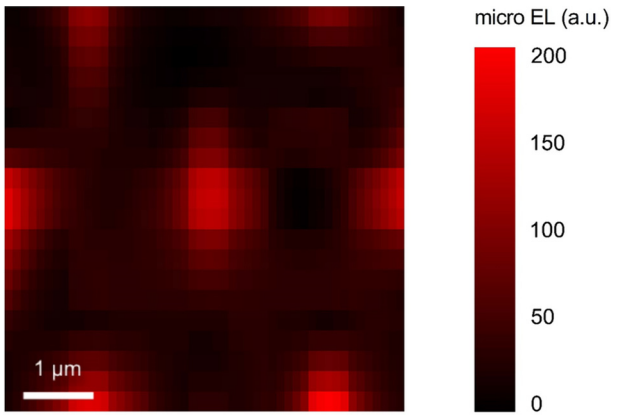

FIG. 4. Micro electroluminescence mapping of hexagonally arranged mesoscopic p-GaN/$In_{0.9}Ga_{0.1}N$/n-GaN nano-LED elements. The results demonstrate a uniform distribution in optical properties over a large area in the array. The mapping is recorded with an InGaAs detector at a wavelength of 1550 nm and the stage moves in 500 nm-sized steps.

nano-LED structures etched from LED layers on sapphire substrate that the EL peak wavelength does correlate with the structure size[23] and a red-shift of electroluminescence wavelength is observed as the structure dimensions decrease. Extensive earlier photoluminescence studies[24] disclosed that the emission wavelength for tensile strained GaN layers deposited on Si tends to blue shift and compressive strained GaN on sapphire tends to red shift as the structure sizes become smaller in reactive ion etching processes. The emission wavelength ultimately coincides for GaN deposited on both templates as the nanostructure dimension decreases. This is attributed to the possibility of strain relaxation in the etched structures.[24] For the nano-LED devices reported here, the same behavior is observed. We found that a single nano-LED with a diameter of 20 nm exhibits about 100 nm redshift in comparison to its 100 nm diameter counterpart (Figure 5). There have been a number of reports dealing with the optical and structural characteristics of InAs quantum dots deposited by self-assembly in a Stranski-Krastanov growth mode on GaAs substrates (see e.g., Refs. 25 and 26). It was found that there is a non-uniform distribution of strain in the structures, which strongly affects their emission energy. The InAs

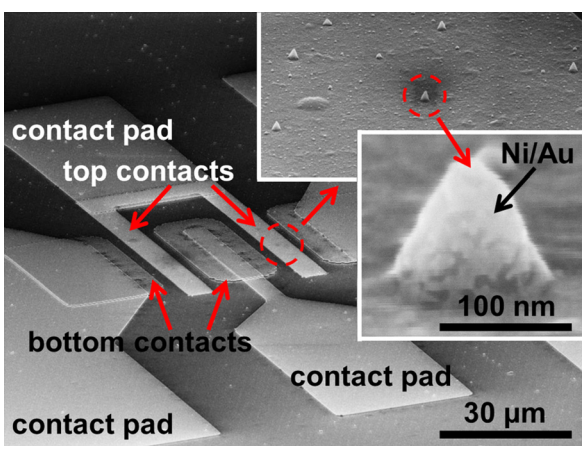

FIG. 3. Scanning electron micrograph of integrated p-GaN/$In_{0.9}Ga_{0.1}N$/n-GaN p-i-n nanostructures. The inset shows the hexagonally arranged structures and a single nanopyramid with Ni/Au top contact.

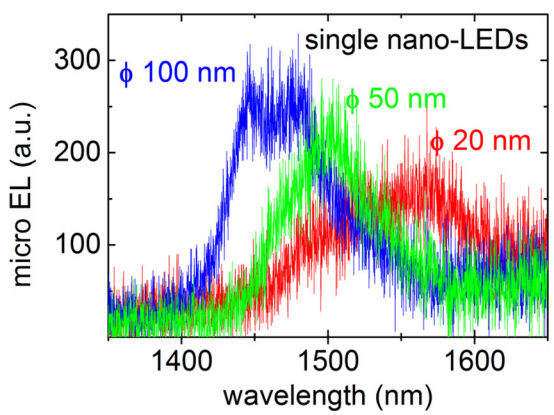

FIG. 5. Micro electroluminescence measurements for single 20 nm, 50 nm, and 100 nm (diameter) vertically integrated p-GaN/$In_{0.9}Ga_{0.1}N$/n-GaN nano-LED structures. The nano-LED diameter size can be used additionally to tune the emission wavelength.[23]

quantum dots (pyramids) were encompassed in GaAs layers. The effect of strain during nanostructure growth and its influence on emission properties is probably different for the nanostructures reported here. At first, the structures fill the holes in the mask. As soon as the nanostructures exceed the mask, they may relax. A formation of crystal defects may be less likely than in layer structures. This effect was already observed for pure GaN and InN nanopyramids deposited selectively on GaN growth templates.[14,27] Beside the strain due to lattice parameter differences between InGaN and GaN and the resulting difference in size related strain relaxation, an interaction between the mask and nanostructure is also possible, which will be dissimilar at growth temperature and room temperature due to the difference in thermal expansion coefficients of the mask and InGaN alloy. In addition, there may also be a strain effect between the p-doped GaN cap-layer and the InGaN mesostructures even though strain relaxation may be easier towards the top of the nano-LED structure, since there is "room" for relaxation. At any rate, the same systematic size effect of the nanostructures on emission wavelength is observed for the InGaN alloy as for the InN and GaN binary nanostructures. Therefore, the effect is most probably due mainly to strain differences between the respective nanopyramid and growth template as the structure size becomes smaller. An additional strain effect of the p-doped GaN cap will also be present but may be less dominant since the mesostructures are only capped thinly and strain at the top of the mesostructures may relax more efficiently. The effect of mesostructured size can be used to tune the wavelength emission additionally.[23]

At last, nano-LEDs were subjected to an ultimate "stress test." Usually, in future, the emitters are to be operated in a pulsed regime. In contrast, here, we investigated their long-term operation stability by driving them constantly at 4 V bias. To this end, we recorded the individual spectra (representative spectra are presented in Figure 5) for the 3 different nano-LED sizes for 1000 h (Figure 6). Ideally, a constant EL intensity would be desirable. However, the intensity decreases moderately for all three diameter sizes—somewhat earlier for the smaller than for the larger devices. For the mesoscopic-sized structures, a larger decline of intensity is found, at first. However, after this initial stronger decrease, the intensity of the EL only diminishes slightly with time. Even the mesoscopic structures were driven for up to 1000 h. After the "stress test," the electroluminescence resumed its initial intensity indicating that the nano-LEDs do not deteriorate and heating effects most probably account for the intensity decrease. Furthermore, our mesoscopic InGaN structures (depending on diameter) feature a very low power consumption in the range between 2 nW and 30 nW.

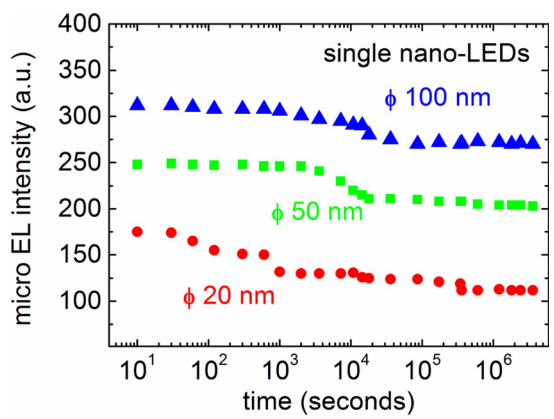

FIG. 6. Reliability measurements for vertically intergrated p-GaN/$In_{0.9}Ga_{0.1}N$/n-GaN nano-LED structures with a diameter of 20 nm, 50 nm, and 100 nm—micro EL intensity measured for 1000 h at 4 V bias. The intensity decreases only moderately with time.

We integrated mesoscopic p-GaN/$In_{0.9}Ga_{0.1}N$/n-GaN structures into a vertical device layout suitable for DC testing and future high frequency operation. They emit within the telecommunication wavelength range. It was demonstrated that the technological process for the nano-LED emitters is well suitable for long-term operation without any indication of significant degradation effects. They feature a very low-energy consumption in the range of 2 nW–30 nW. This nano-LED technology is suitable for low energy consumption optoelectronics operated in the telecommunication wavelength range.

The German Ministry for education and research (BMBF) is acknowledged for financial support within the Project Nos. EPHQUAM (16BL0904) and QPENS (13N9898).

[1]A. Kikuchi, M. Kawai, M. Tada, and K. Kishino, Jpn. J. Appl. Phys., Part 2 **43**, L1524 (2004).
[2]H.-M. Kim, Y.-H. Cho, H. Lee, S. Il Kim, S. R. Ryu, D. Y. Kim, T. W. Kang, and K. S. Chung, Nano Lett. **4**, 1059 (2004).
[3]S. Li and A. Waag, J. Appl. Phys. **111**, 071101 (2012).
[4]G. S. Buller and R. J. Collins, Meas. Sci. Technol. **21**, 012002 (2010).
[5]Ł. Dusanowski, M. Syperek, P. Mrowiński, W. Rudno-Rudziński, J. Misiewicz, A. Somers, S. Höfling, M. Kamp, J. P. Reithmaier, and G. Sęk, Appl. Phys. Lett. **105**, 021909 (2014).
[6]R. Mathew, H. Y. S. Yang, and K. C. Hall, Phys. Rev. B **92**, 155306 (2015).
[7]R. Mathew and K. C. Hall, Phys. Status Solidi **13**, 67 (2016).
[8]A. Winden, M. Mikulics, A. Haab, D. Grützmacher, and H. Hardtdegen, Jpn. J. Appl. Phys., Part 1 **52**, 08JF05 (2013).
[9]M. Mikulics, M. Kočan, A. Rizzi, P. Javorka, Z. Sofer, J. Stejskal, M. Marso, P. Kordoš, and H. Lüth, Appl. Phys. Lett. **87**, 212109 (2005).
[10]M. Mikulics, M. Marso, P. Javorka, P. Kordoš, H. Lüth, M. Kočan, A. Rizzi, S. Wu, and R. Sobolewski, Appl. Phys. Lett. **86**, 211110 (2005).
[11]M. Mikulics, P. Kordos, D. Gregusova, R. Adam, M. Kocan, S. Wu, J. Zhang, R. Sobolewski, D. Grutzmacher, and M. Marso, IEEE Photonics Technol. Lett. **23**, 1189 (2011).
[12]M. A. Reshchikov, F. Shahedipour-Sandvik, B. J. Messer, V. Jindal, N. Tripathi, and M. Tungare, Phys. B: Condens. Matter **404**, 4903 (2009).
[13]A. Winden, M. Mikulics, D. Grützmacher, and H. Hardtdegen, Nanotechnology **24**, 405302 (2013).
[14]A. Winden, M. Mikulics, T. Stoica, M. von der Ahe, G. Mussler, A. Haab, D. Grützmacher, and H. Hardtdegen, J. Cryst. Growth **370**, 336 (2013).
[15]H. Hardtdegen, M. Hollfelder, R. Meyer, R. Carius, H. Münder, S. Frohnhoff, D. Szynka, and H. Lüth, J. Cryst. Growth **124**, 420 (1992).
[16]H. Hardtdegen, M. Pristovsek, H. Menhal, J.-T. Zettler, W. Richter, and D. Schmitz, J. Cryst. Growth **195**, 211 (1998).
[17]Y. S. Cho, H. Hardtdegen, N. Kaluza, N. Thillosen, R. Steins, Z. Sofer, and H. Lüth, Phys. Status Solidi **3**, 1408 (2006).
[18]H. Hardtdegen, N. Kaluza, R. Schmidt, R. Steins, E. V. Yakovlev, R. A. Talalaev, Y. N. Makarov, and J.-T. Zettler, Phys. Status Solidi **201**, 312 (2004).
[19]I. Vurgaftman and J. R. Meyer, J. Appl. Phys. **94**, 3675 (2003).
[20]R. R. Pelá, C. Caetano, M. Marques, L. G. Ferreira, J. Furthmüller, and L. K. Teles, Appl. Phys. Lett. **98**, 151907 (2011).
[21]L. G. Ferreira, M. Marques, and L. K. Teles, Phys. Rev. B **78**, 125116 (2008).
[22]S. Riess, M. Mikulics, A. Winden, R. Adam, M. Marso, D. Grützmacher, and H. Hardtdegen, Jpn. J. Appl. Phys., Part 1 **52**, 08JH10 (2013).
[23]M. Mikulics and H. Hardtdegen, Nanotechnology **26**, 185302 (2015).

[24]N. Thillosen, K. Sebald, H. Hardtdegen, R. Meijers, R. Calarco, S. Montanari, N. Kaluza, J. Gutowski, and H. Lüth, Nano Lett. **6**, 704 (2006).
[25]R. Heitz, M. Grundmann, N. N. Ledentsov, L. Eckey, M. Veit, D. Bimberg, V. M. Ustinov, A. Y. Egorov, A. E. Zhukov, P. S. Kop'ev, and Z. I. Alferov, Surf. Sci. **361–362**, 770 (1996).
[26]M. Grundmann, O. Stier, and D. Bimberg, Phys. Rev. B **52**, 11969 (1995).
[27]A. Winden, M. Mikulics, A. Haab, T. Stoica, M. von der Ahe, K. Wirtz, H. Hardtdegen, and D. Grützmacher, Phys. Status Solidi **9**, 624 (2012).